ISIJ International, Vol. 54 (2014), No. 9, pp. 2089–2096

Influence of High Temperature Interaction between Sinter and Lump Ores on the Formation Behavior of Primary-slags in Blast Furnace

Xinliang LIU, Shengli WU,* Wei HUANG, Kaifa ZHANG and Kaiping DU

School of Metallurgical and Ecological Engineering, University of Science and Technology Beijing, Beijing, 100083 China.

(*Received on January 25, 2014; accepted on May 29, 2014*)

The primary-slags formation behaviors of sinter, lump ores and integrated burdens were studied to explore the high temperature interaction between sinter and lump ores in blast furnace. The results showed that the softening and melting properties of lump ores, viscosity and fluidity index of primary-slags of lump ores would be improved by the high temperature interaction. Particularly, the high temperature interaction was influenced by the chemical composition and porosity of iron ore samples. The high temperature interaction between sinter and lump ore L-2 (a typical limonite lump ore from Australia) was much stronger. Though the high temperature properties of lump ore L-2 was much worse than lump ore L-1 (a typical hematite lump ore from South Africa), the high temperature properties of integrated burden B (consist of sinter and lump ore L-2) was not worse than that of integrated burden A (consist of sinter and lump ore L-1) due to the strong high temperature interaction. In addition, the suitable MgO/Al_2O_3 weight ratio was calculated based on the assumption that the only phases of slags were akermanite and gehlenite, which showed a decreasing tend with the increase of CaO/SiO_2 weight ratio.

KEY WORDS: primary-slags; high temperature interaction; formation behavior; fluidity index; mechanism.

1. Introduction

Through the dissection of blast furnace, researchers have found that the shape and thickness of cohesive zone have significant influence on the blast furnace operation. While, the high temperature properties of blast furnace slags play an important role on the softening and melting behavior of raw materials in blast furnace.[1,2] Many researchers have found that the chemical composition, such as CaO/SiO_2, Al_2O_3 and MgO content, have great influence on the fluidity and viscosity of blast furnace slags.[3–5] On the other hand, researchers also found that the sinter of high basicity would interact with lump ores or pellets at high temperature, the softening and melting properties of lump ores or pellets would be improved by the high temperature interaction.[6–9]

However, though various studies are conducted to research the properties of blast furnace slags, no satisfactory knowledge has been acquired about the influence of high temperature interaction on the primary-slags formation behaviors in blast furnace. Because the mixture between sinter and lump ores in blast furnace was not simply physical mixing, it is of great significance to study the primary-slags formation behaviors of respective iron ores and integrated burdens to explore the mechanism of high temperature interaction.

In the present work, the primary-slags formation behaviors of respective iron ores (sinter and lump ores) and integrated burdens (consist of sinter and lump ores) were studied. The chemical compositions, fluidity index, viscosity and liquidus temperature of primary-slags were also studied. Besides, the mechanism and influencing factors of high temperature interaction was also discussed.

2. Experimental

2.1. Raw Materials

Raw materials used in this work were sinter and lump ores, S-1 is sinter of high basicity from China, L-1 is a typical hematite lump ore from South Africa, L-2 is a typical limonite lump ore from Australia, all these raw materials are in actual use for blast furnace in China. Two integrated burdens are designed to study the influence of high temperature interaction. The compositions of integrated burden are determined to keep the basicity of final slags constant at 1.20 through the chemical balance. The chemical compositions of respective iron ores and integrated burdens are shown in **Table 1** and the compositions of designed integrated burdens are shown in **Table 2**.

According to the chemical composition of integrated burdens and respective iron ores, it is found that the iron grade of lump ore L-1 is much higher than that of others. The iron grade content of lump ore L-2 is lowest, while the Al_2O_3 and SiO_2 content of lump ore L-2 is highest. Particularly, obvious pores could be observed on the surface of lump ore L-2.

* Corresponding author: E-mail: wushengli@ustb.edu.cn
DOI: http://dx.doi.org/10.2355/isijinternational.54.2089

Table 1. Chemical compositions of iron ore samples (wt%).

Samples	TFe	FeO	CaO	SiO_2	Al_2O_3	MgO	TiO_2	P	S
S-1	57.43	8.24	9.41	4.98	1.76	1.66	0.10	0.061	0.013
L-1	66.57	0.69	0.21	4.37	1.01	0.02	0.04	0.034	0.007
L-2	57.40	1.20	0.38	5.10	2.61	0.01	0.04	0.020	0.018
Integrated burden A	59.46	6.36	7.12	4.83	1.57	1.25	0.08	0.054	0.012
Integrated burden B	57.42	6.64	7.36	5.01	1.95	1.29	0.09	0.051	0.014

Table 2. Compositions of integrated burdens.

Samples	Proportions of respective iron ores/wt%
Integrated burden A	75.12% S-1 + 24.88% L-1
Integrated burden B	77.34% S-1 + 22.66% L-2

2.2. Experimental Procedures

The primary-slags formation experiments are taken by the softening-melting equipment and the schematic diagram of the softening-melting equipment is illustrated in **Fig. 1**. Samples having a layer thickness of 65 mm were charged in a graphite crucible and cokes with a layer thickness of 20 mm were placed over and below the iron ore samples. The iron ore samples are 10–12.5 mm in diameter and the cokes are 6.3–10 mm in diameter. Subject to the condition of constant layer thickness, the charge of the iron ore samples weighted different due to the difference of density. The inner diameter of the graphite crucible is about 48 mm.

Experimental conditions for the primary-slags formation behavior are shown in **Fig. 2**. The heating up rate is 10°C/min below 900°C and 5°C/min over 900°C. Especially, the samples are kept at 900°C for 60 min to make sure the iron ore samples are adequately reduced. Gas flow is 5 L/min of N_2 blow 500°C and 12 L/min of reducing gas over 500°C, the composition of reducing gas is $CO:N_2=30:70(\%)$. The load of 0.1 MPa is added to the samples when the temperature reaches 500°C. After the primary-slags formation test, the samples are cooled down to room temperature by N_2 with the flow rate 5 L/min. The reason why the samples are cooled by continuous cooling is that rapid quenching method is impossible to apply in the softening-melting equipment, as it is not allowable to take out the samples in several seconds due to the high temperature.

A typical set of primary-slags formation test results of sinter is shown in **Fig. 3**, in which pressure drop, temperature and shrinkage rate are conducted to evaluate the primary-slags formation behaviors of iron ore samples. It is difficult to observe the behavior directly as the internal of the softening-melting equipment is not visible. Then some indexes are conducted to evaluate the primary-slags formation behavior of iron ores. T_s is the temperature when the pressure drop of the samples reaches 0.2 kPa, indicating primary-slags start to produce. T_m is the temperature when the pressure drop begin to quickly increase (T_m is the temperature when the slope of pressure drop-time curve reaches 0.15 kPa/min in this work), meaning the primary-slags produce rapidly. T_p is the temperature when the pressure drop of the samples reaches the highest (ΔP_{max}), meaning the primary–slags are totally produced. Besides, the temperature range (T_p-T_s) reflects the formation temperature interval of primary-slags.

The influence of high temperature interaction on the softening and melting properties of iron ores samples is also studied. While, softening start temperature ($T_{10\%}$) is the tem-

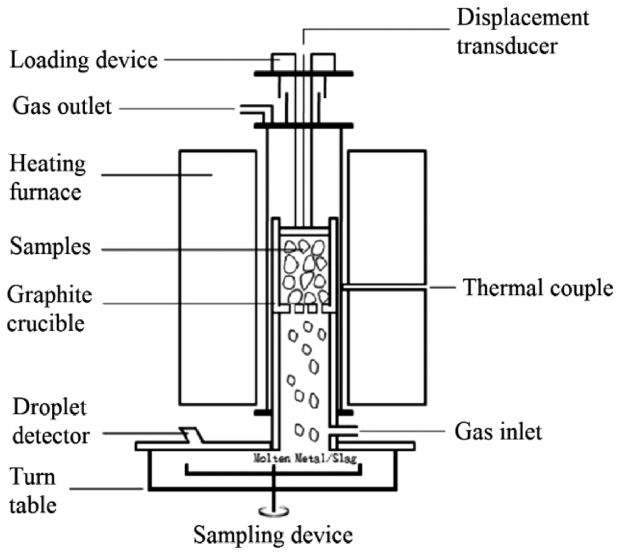

Fig. 1. Schematic diagram of softening-melting equipment.

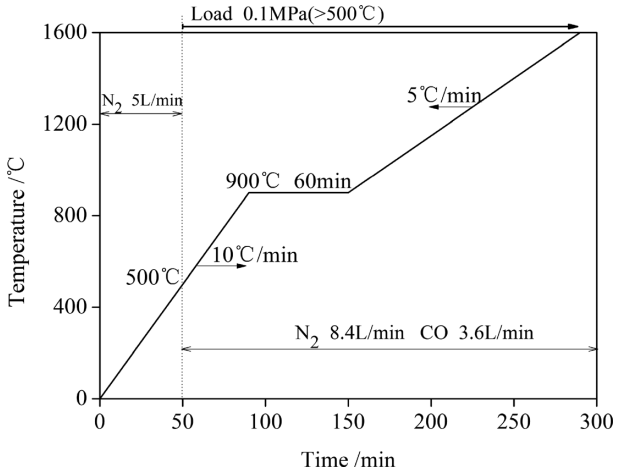

Fig. 2. Experimental conditions for primary-slags formation behavior.

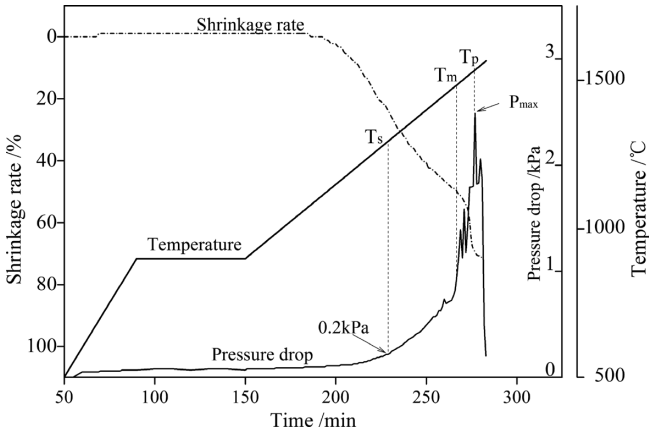

Fig. 3. A typical set of primary-slags formation behavior for sinter.

perature when the shrinkage of the samples reaches 10%, softening end temperature ($T_{40\%}$) is the temperature when the shrinkage of the samples reaches 40%. The temperature interval ($T_{40\%}$-$T_{10\%}$) represents the softening zone of iron ore samples. T_d is the temperature at which dripping starts and the temperature interval (T_d-$T_{10\%}$) reflect the thickness of the cohesive zone. The S-value is an integrated pressure drop value over the cohesive zone and the maximum pressure drop ΔP_{max}.

To study the whole process of the high temperature behaviors of iron ores and gain the primary-slags at T_p, every test contains two steps. Firstly, the whole process of iron ore samples from room temperature to dripping finished is conducted. Secondly, stop heating the samples at T_p and cool down the samples to room temperature under the protection of pure N_2.

To evaluate the influence of high temperature interaction between sinter and lump ores, the high temperature interaction index (INI) is proposed, which also indicating the abilities of high temperature interaction to improve the poor softening and melting properties of lump ores. The formula of INI is as follows:

$$INI = \frac{(a\mu_1 + b\mu_2) - \mu_0}{a\mu_1 + b\mu_2} \times 1 \quad \text{..... (1)}$$

where, μ_0: the cohesive zone temperature interval of integrated burden, μ_1: the cohesive zone temperature interval of respective sinter, μ_2: the cohesive zone temperature interval of lump ores, a: the proportion of sinter in integrated burdens, b: the proportion of respective lump ores in integrated burdens.

The projection area method[10,11] is used to study the fluidity index of primary-slags. The fluidity index of primary-slags is defined as the increase of vertical projection area after melt primary-slags flowed. **Figure 4** shows the schematic diagram of projection area method. As shown in formula (2), the fluidity index is calculated.

$$Fluidity\ Index = (A_{after} - A_{before}) / A_{before} \quad \text{..... (2)}$$

Where, A_{after} is the vertical projection area of primary-slags after melting, A_{before} is the vertical projection area of primary-slags before melting.

Particularly, the primary-slags samples used for fluidity index test are prepared from reagent-grade chemicals such as CaO, Al_2O_3, MgO, FeO and SiO_2. These oxides are crushed into fine power and well mixed at the composition determined by the X-ray Fluorescence Spectrometer (XRF) results of primary-slags.

3. Results

3.1. Softening and Melting Properties

The results of the softening and melting properties of sinter, lump ores and integrated burdens were shown in **Table 3**. The lump ores have really poor softening and melting properties,[12,13] started softening at low temperature and dripping at high temperature with high pressure drop. While the dripping start temperature of sinter was the highest (1 551°C), which was also bad for the blast furnace operation. However, the softening and melting properties of integrated burdens were quite better than that of respective iron ores,[8,14] the softening start temperature of integrated burdens

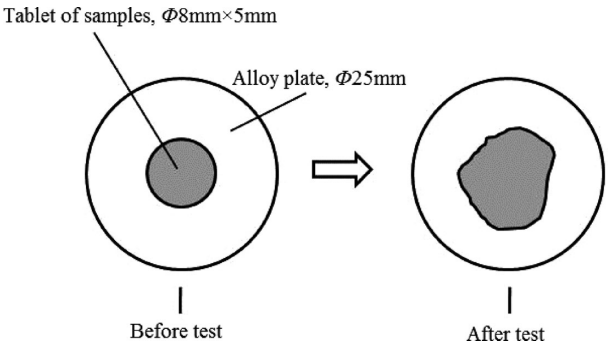

Fig. 4. Schematic diagram of fluidity of primary-slags.

Table 3. Softening and melting properties of iron ore samples.

Samples	$T_{10\%}$/ °C	$T_{40\%}$/ °C	$T_{40\%}$-$T_{10\%}$/ °C	T_d / °C	T_d-$T_{10\%}$/ °C	ΔP_{max}/ kPa	S/kPa·°C
S-1	1 199	1 317	118	1 551	352	2.54	120
L-1	1 117	1 302	185	1 508	391	2.90	121
L-2	904	1 072	168	1 529	625	3.62	147
A	1 157	1 288	131	1 483	326	2.12	98
B	1 163	1 282	119	1 496	333	2.53	97

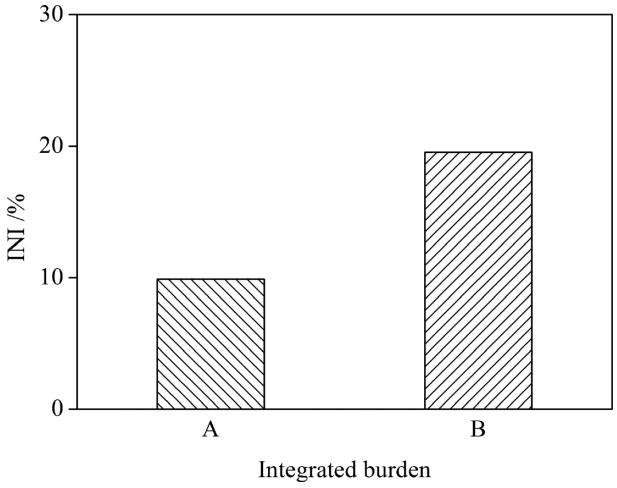

Fig. 5. INI indexes between sinter and lump ores.

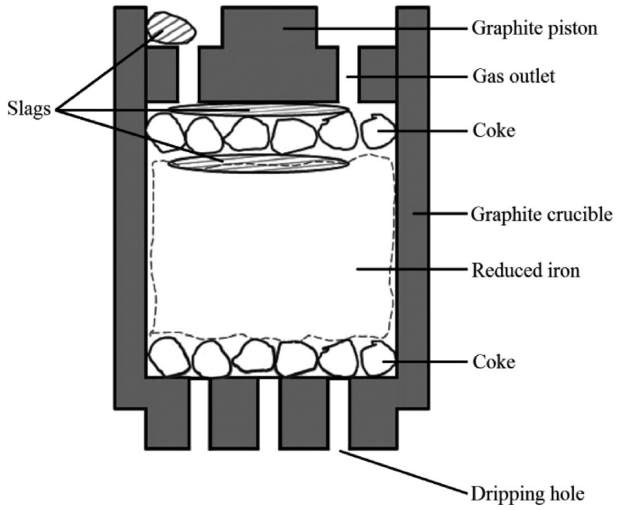

Fig. 6. Schematic diagram of primary-slags distribution after test.

were higher than that of lump ores and lower than sinter. Moreover, the dripping temperature, ΔP_{max} and the S-value of integrated burdens were all lower than respective sinter and lump ores. This results agreed with the former results studied by Higuchi *et al.*,[15] that is the dripping temperature would increase with basicity from 1.1 to 2.5. Besides, the softening and melting properties of lump ore L-2 was the worst, one probable reason could be that the high porosity leading lump ore L-2 very easy to reduce, making lump ore L-2 softened at very low temperature.[16]

Compared with respective iron ores, the softening and melting temperature intervals of integrated burdens were much narrower, proving that sinter and lump ores were not physically mixed in blast furnace. **Figure 5** shows the INI indexes of high temperature interaction between sinter and lump ores. Generally speaking, the INI index between sinter and lump ore L-2 was much higher than that between sinter and lump ore L-1. This result explained the above phenom-

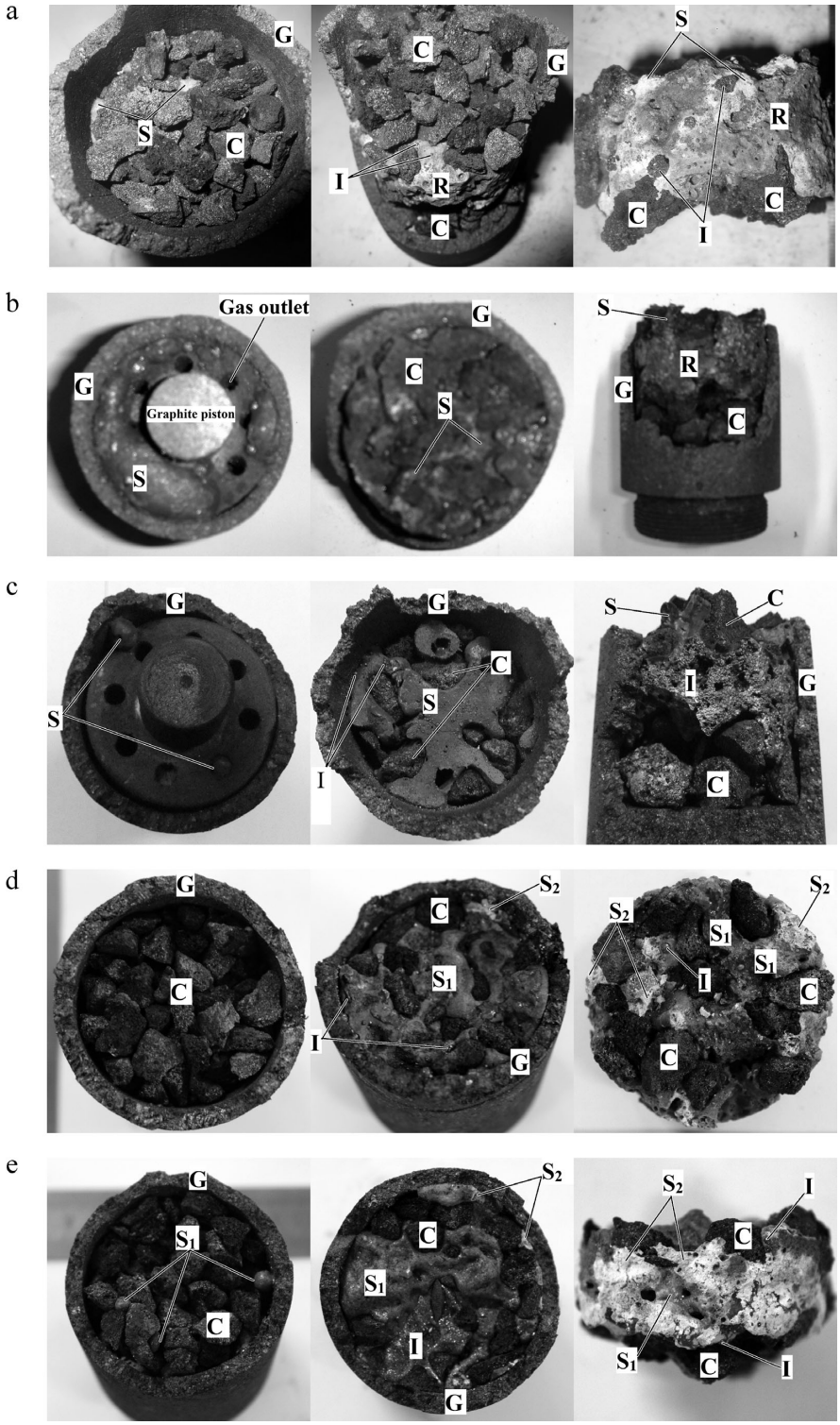

Fig. 7. Primary-slags distribution of iron ores samples. a, b and c showed the primary-slags distributions of S-1, L-1 and L-2 respectively; d and e showed primary-slags distribution of integrated burden A and B respectively. G: Graphite crucible side, C: Coke, I: Iron, R: Reduced iron ores, S: Primary-slags of respective iron ores, S1: Primary-slags produced by interaction between sinter and lump ores, S2: Primary-slags of respective sinter.

enon why the softening and melting properties of integrated burden B was not worse than integrated burden A, though the high temperature properties of lump ore L-2 was the worst.

3.2. Primary-slags Formation Behaviors

To study the properties of primary-slags, stopped heating when the pressure drop reached the highest (ΔP_{max}) and cooled down the samples to room temperature by N_2 with the flow rate 5 L/min. **Figure 6** shows the schematic diagram of samples in the graphite crucible after test and the distribution of primary-slags, reduced iron ores and cokes at T_p.

Figure 7 shows the photos of primary-slags distribution of respective iron ores and integrated burdens. As shown in the photos, flooding phenomena were observed in all primary-slags of respective iron ores and the flooding phenomena of lump ores are much heavier. However, no obvious flooding phenomena were observed in the integrated burdens. The reason could be that the high temperature interaction between sinter and lump ores improved the high temperature properties of primary-slags, such as liquidity and viscosity. Particularly, the primary-slags of integrated burdens consisted of two parts based on the results of XRD and XRF analysis, most part of the primary-slags were formed by the high temperature interaction between sinter and lump ores (marked as S_1 in the photo d and e), which were gray as shown in Fig. 7. While small part of the primary-slags were formed by sinter (marked as S_2 in the photos d and e), and this part of primary-slags were white and in shape of powder as shown in Fig. 7. This was that because not all sinters interacted with lump ores and the rest sinter ores would also produce primary-slags.

Figure 8 shows the primary-slags formation temperature intervals of iron ore samples. For the respective iron ores, the primary-slags starting and finishing formation temperatures of lump ores were lower than sinter. While the primary-slags formation temperature interval of lump ore L-2 was extremely wide, the intervals of lump ore L-1 and sinter S-1 were almost the same. For the integrated burdens, the primary-slags starting and finishing formation temperatures of integrated burden B were higher than integrated burden A, but the formation temperature interval of integrated burden A was about 10°C narrower than integrated burden B. However, the primary-slags starting formation temperature of integrated burdens were higher than lump ores and lower than sinter, while the formation temperature intervals of integrated burden were much narrower than all respective iron ores. These results indicated that the high temperature interaction could improve the primary-slags formation behaviors but the improvement varies with different kinds of lump ores.

The primary-slags were analyzed though X-ray Fluorescence Spectrometer (XRF) after the slags samples were ground less than 200 meshes, and the chemical compositions (only take FeO, CaO, SiO_2, Al_2O_3 and MgO into account) of primary-slags were shown in **Table 4**. It can be seen from the table that the primary-slags FeO content of lump ores were more than 16%, but the FeO content of integrated burdens were less than 4%. While the primary-slags Al_2O_3 content of lump ores were higher than other samples, and the primary-slags Al_2O_3 content of lump ore L-2 even closed to 24%. Besides, the SiO_2 content of lump ores were all over 50%. All these difference would influence the high temperature properties of primary-slags, such as fluidity index, viscosity and so on.

Figure 9 shows the fluidity indexes of primary-slags measured by the projection area method at 1 450°C. The fluidity index of sinter was failed to measure as the primary-slags were in shape of powder after test due to the crystal transformation of $2CaO{\cdot}SiO_2$ in the process of cooling, thus the projection area of powder was doubtful because it could be influenced by the N_2 airflow. However, the fluidity index of lump ore L-2 was higher than lump ore L-1 in spite the Al_2O_3 content of lump ore L-2 was much higher. As for the

Table 4. Primary-slags chemical composition of iron ore samples.

Samples	FeO/ wt%	CaO/ wt%	SiO_2/ wt%	Al_2O_3/ wt%	MgO/ wt%	R_2	R_4
S-1	7.60	49.74	26.51	9.31	6.84	1.88	1.58
L-1	16.33	2.65	63.72	16.76	0.54	0.04	0.04
L-2	18.61	1.92	54.71	23.59	1.17	0.04	0.04
A	3.27	50.68	28.69	10.87	6.49	1.77	1.45
B	1.06	49.63	30.01	12.25	7.05	1.65	1.34

R_2 was the weight ratio of CaO/SiO_2, R_4 was the weight ratio of $(CaO+MgO)/(SiO_2+Al_2O_3)$

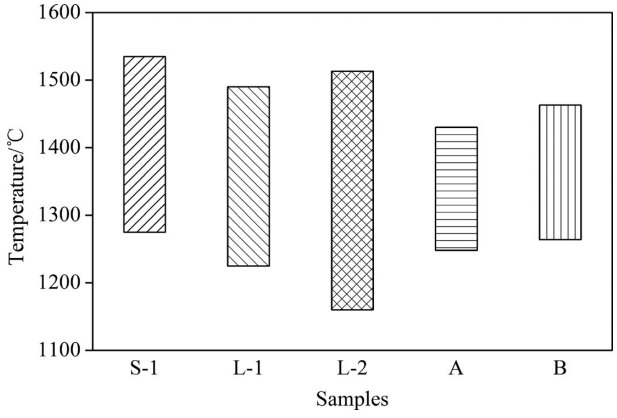

Fig. 8. Formation temperature intervals of primary-slags.

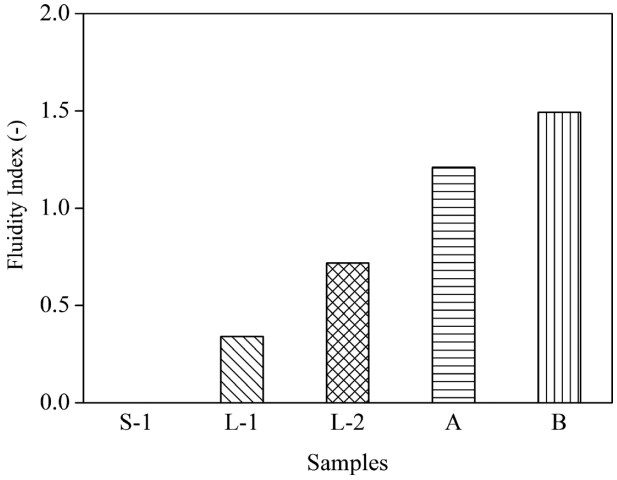

Fig. 9. Fluidity indexes of primary-slags at 1 450°C.

integrated burdens, the fluidity index of integrated burden B was higher than integrated burden A. What is more, the fluidity indexes of integrated burdens were all higher than that of respective lump ores.

Figure 10 shows the liquidus temperature of primary-slags calculated by the thermodynamic calculation software FactSage based on the chemical compositions results of XRF. **Table 5** shows the liquid ratio, liquid phase composition and liquid viscosity of primary-slags calculated by FactSage at 1 450°C. As shown in the picture, the liquidus temperatures of integrated burdens were much higher than respective iron ores, which were all over 1 600°C. The liquidus temperature of lump ores was much lower than sinter. According to the calculated results by FactSage, the liquid ratio of sinter, integrated burden A and integrated burden B were 83.05%, 83.05% and 87.60%, respectively. The solid phase of primary-slags at 1 450°C was mainly $2CaO{\cdot}SiO_2$

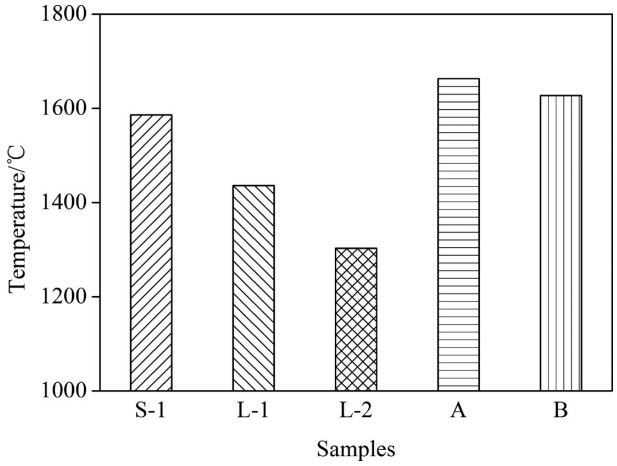

Fig. 10. Liquidus temperature of primary-slags.

Table 5. Liquid composition and viscosity of primary-slags at 1 450°C.

Samples	Liquid ratio/ %	Liquid composition /wt%					Solid phase	Liquid Viscosity/ Pa·s
		FeO	CaO	SiO_2	Al_2O_3	MgO		
S-1	83.05	8.88	47.56	25.31	11.21	7.04	$2CaO{\cdot}SiO_2$	0.136
L-1	100.00	16.33	2.65	63.72	16.76	0.54	–	51.520
L-2	100.00	18.61	1.92	54.71	23.59	1.17	–	11.120
A	83.05	3.94	47.73	27.43	13.09	7.81	$2CaO{\cdot}SiO_2$ $3CaO{\cdot}MgO{\cdot}2SiO_2$	0.176
B	87.60	1.21	47.44	29.32	13.98	8.05	$2CaO{\cdot}SiO_2$	0.210

except integrated burden A contained part of $3CaO{\cdot}MgO{\cdot}2SiO_2$. In addition, the liquid viscosity of sinter and integrated burdens were all less than 0.22 Pa·s, but the liquid viscosity of lump ores were all over 11 Pa·s. All these results indicated that the high temperature properties of primary-slags of integrated burdens were better than that of respective lump ores.

To further study the influence of high temperature interaction between sinter and lump ores, the primary-slags samples of sinter S-1, lump ore L-2 and the integrated burden B were analyzed through X-Ray diffraction and scanning electron microscope analysis because the high temperature interaction between sinter S-1 and lump ore L-2 was much stronger. **Figure 11** shows the diffraction patterns of primary-slags. The primary-slags phases of lump ore L-2, sinter S-1 and integrated burden B were quite different with each other. The main primary-slags phases of lump ore L-2 were mullite ($3Al_2O_3{\cdot}2SiO_2$), fayalite ($2FeO{\cdot}SiO_2$) and SiO_2. While $2CaO{\cdot}SiO_2$, merwinite ($3CaO{\cdot}MgO{\cdot}2SiO_2$) and gehlenite ($2CaO{\cdot}Al_2O_3{\cdot}SiO_2$) were observed from the X-ray diffraction results of sinter. However, the main primary-slags phases of integrated burden B were akermanite ($2CaO{\cdot}MgO{\cdot}2SiO_2$), gehlenite ($2CaO{\cdot}Al_2O_3{\cdot}SiO_2$) with little $2CaO{\cdot}SiO_2$ and mullite ($3Al_2O_3{\cdot}2SiO_2$). As mentioned above, it was difficult to quench the samples in the softening-melting equipment. The cooling method should somewhat affect the phases composition of the primary-slags. However, some researchers had studied the crystallization behaviors of blast furnace slags under continuous cooling

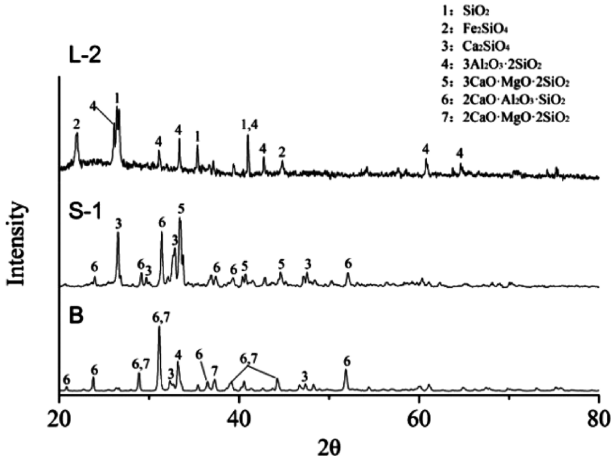

Fig. 11. X-ray diffraction analysis of S-1, L-2 and integrated burden B.

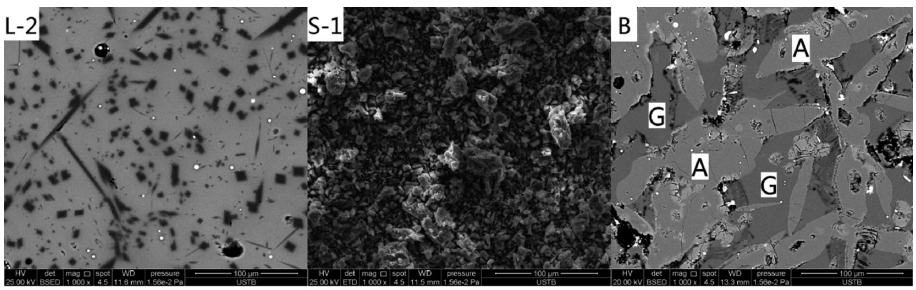

(a) (b) (c)

Fig. 12. Primary-slags microstructures of L-2, S-1 and integrated burden B. (a): Dark phase and grey phase are mullite, fayalite mixed with quartz, respectively. (b): The primary-slags of sinter are in shape of powder. (c): G: Gehlenite, A: Akermanite.

and quenching method. Kashiwaya *et al.* found that the slags began crystallize less than 10 s from 1 000 to 1 300°C.[17] While merwinite, gehlenite and akermanite were found to be the main phases of the blast furnace slags under both continuous cooing method and quenching method,[18–20] which was similar to the results of the present work.

Figure 12 shows the SEM pictures of lump ore L-2, sinter S-1 and integrated burden B after continuous cooling. The microstructure of integrated burden was quite different with respective sinter and lump ore. The primary-slags phase distribution of lump ore L-2 were fayalite, mullite and quartz mixed together, while the primary-slags of sinter S-1 were in shape of powder because of the crystal transformation of $2CaO{\cdot}SiO_2$ in the process of cooling. The primary-slags microstructure of integrated burden B was gehlenite intertwined with akermanite.

4. Discussion

4.1. Primary-slags Formation Behaviors of Respective Lump Ores and Sinter

From the above results, we could obtain the conclusion that sinter and lump ores are not physically mixed together and the high temperature interaction would change the high temperature properties of primary-slags, such as fluidity index, viscosity, and phase composition. The primary-slags formation behaviors of sinter, lump ore and integrated burden were discussed to study the high temperature interaction between sinter and lump ores.

As for lump ores, the Fe_2O_3 were gradually reduced and primary-slags were formed during the reducing process. The main chemical compositions of the primary-slags were FeO, SiO_2 and Al_2O_3 as lump ores contained little CaO and MgO. Meanwhile, according to the phase diagram of Al_2O_3–SiO_2–FeO[21] and XRD analysis results, the initial phase in the primary-slags should be fayalite ($2FeO{\cdot}SiO_2$). While with the further reduction of lump ores, new phases such as mullite ($3Al_2O_3{\cdot}2SiO_2$) and SiO_2 were produced as FeO content decreased with the reduction of lump ores.

As for sinter, the initial phase of the primary-slags should also contain fayalite ($2FeO{\cdot}SiO_2$) and the content of fayalite was limited as the SiO_2 content of sinter was quite lower, but other phases such as wollastonite (β-(Ca,Fe)O·SiO_2) and olivine (2(Fe,Ca)O·SiO_2) would be formed based on the phase diagram of CaO–FeO–SiO_2.[8,22] However, with the decrease of FeO content in primary-slags of sinter, new phase of primary-slags were produced according to the XRD analysis results, such as $2CaO{\cdot}SiO_2$, merwinite ($3CaO{\cdot}MgO{\cdot}2SiO_2$) and gehlenite ($2CaO{\cdot}Al_2O_3{\cdot}SiO_2$).

Conclusively, the difference of primary-slags formation behaviors between lump ores and sinter could be attributed to the different phase composition caused by the difference of chemical composition and microstructure between sinter and lump ores.

4.2. Mechanism of High Temperature Interaction

When sinter mixed with lump ores, the high temperature interaction would change the primary-slags formation behaviors of integrated burdens. The reason for high temperature interaction could be summarized as followed: the primary-slags of sinter had more CaO and SiO_2 than was necessary to from akermanite and gehlenite and the excess of CaO and SiO_2 were then sufficient to form $2CaO{\cdot}SiO_2$.[17] At the same time, the lump ores supplied plenty of Al_2O_3 and SiO_2, and then the excess CaO from sinter would interact with Al_2O_3 and SiO_2 from lump ores at high temperature, thus the primary-slags formation behaviors of integrated burdens would be improved.

However, combined with the present study and the former researches,[7–9] the high temperature interaction between sinter and lump ores could be divided into two steps, first step was the interaction caused by diffusion of Al_2O_3 and SiO_2, and the second step was the interaction caused by the diffusion of CaO and MgO.

Firstly, the Al_2O_3 and SiO_2 would diffuse to the interface between sinter and lump ores, which mainly occurred before 1 150°C.[8,9] And this diffusion would decrease the content of $2FeO{\cdot}SiO_2$ in lump ores and increase the content of 2(Fe,Ca)O·SiO_2 or β-(Ca,Fe)O·SiO_2 in sinter, thus the initial primary-slags phases of integrated burdens would be fayalite, wollastonite and olivine. Secondly, with the increase of temperature, the diffusion of CaO and MgO became more and more obvious, which mainly happened between 1 150°C and 1 300°C.[8,9] While, this diffusion would decrease the content of $2CaO{\cdot}SiO_2$ in sinter and other phases such as merwinite ($3CaO{\cdot}MgO{\cdot}2SiO_2$), akermanite ($2CaO{\cdot}MgO{\cdot}2SiO_2$) and gehlenite ($2CaO{\cdot}Al_2O_3{\cdot}SiO_2$) were produced. Finally, the high melting point phases, such as $2CaO{\cdot}SiO_2$, $3Al_2O_3{\cdot}2SiO_2$ and SiO_2 found in the primary-slags of respective iron ores, decreased due to the high temperature interaction between sinter and lump ores. However, small amounts of mullite ($3Al_2O_3{\cdot}2SiO_2$) and $2CaO{\cdot}SiO_2$ were found in the XRD results of integrated burden B. The reason could be that the high temperature interaction between sinter and lump ores were not completely finished. In addition, no merwinite was found in primary-slags of integrated burden because merwinite was a metastable phase and it would transformed into thermodynamically stable phase corresponding to the phase diagram of the system.[17]

4.3. Influencing Factors of High Temperature Interaction

As the above results showed, sinter of high basicity would interact with lump ores at high temperature. However, the high temperature interaction indexes were quite different between sinter and different lump ores, and the difference could be attributed to the chemical compositions and pore structure except temperature.

4.3.1. Chemical Compositions

The chemical compositions of iron ore samples, such as CaO, SiO_2 and Al_2O_3, were the dominant factors of the high temperature interaction. The concentration gradient of these oxides determined the reaction impetus of high temperature interaction. Generally speaking, the reaction impetus increased with the increase of Al_2O_3 and SiO_2 content of lump ores and CaO content of sinter. However, excessive CaO and SiO_2 would produce $2CaO{\cdot}SiO_2$ and excessive Al_2O_3 and SiO_2 would also increase the viscosity of primary-slags, which was negative for the high temperature properties of primary-slags.

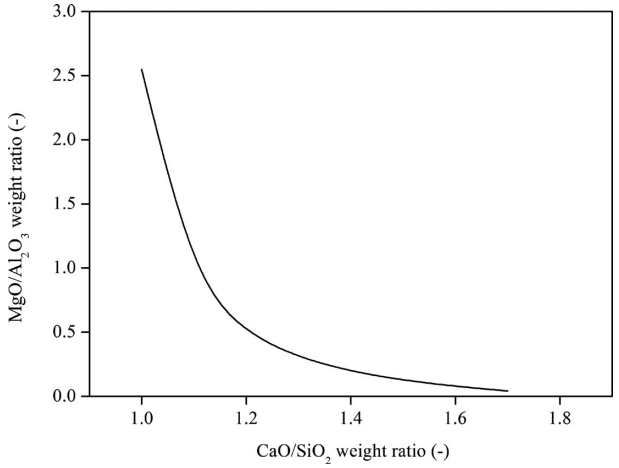

Fig. 13. Suitable MgO/Al_2O_3 weight ratio under different CaO/SiO_2 weight ratio.

4.3.2. Pore Structures

As the difference of chemical compositions between sinter and lump ores offered the reaction impetus for high temperature interaction, the pore structure also had great influence on the high temperature interaction between sinter and lump ores. An probable inference could be as follows: the lump ores with high porosity were easy to reduce, which would result low softening and melting temperature.[16] However, the diffusion rate of reactive oxides in liquid was much higher than solid.[23] Thus the high temperature interaction between sinter and high porosity lump ores would be much faster and stronger due to the higher diffusion rate.

Conclusively, the high temperature interaction index between sinter and lump ore L-2 was much higher than sinter and lump ore L-1, because the porosity, Al_2O_3 content and SiO_2 content of lump ore L-2 was higher. However, excessive Al_2O_3 and SiO_2 would be also negative for the high temperature properties of primary-slags. The akermanite and gehlenite phases were positive to the blast furnace operation based on the above results, and then the MgO/Al_2O_3 weight ratio was calculated based on the assumption that the only phases of primary-slags were akermanite and gehlenite. The procedures were as followed: Firstly, the weight ratio of akermanite/gehlenite under different CaO/SiO_2 weight ratio was calculated as the CaO/SiO_2 weight ratio of akermanite and gehlenite were 0.933 and 1.867, respectively. Secondly, the respective weight ratio of MgO and Al_2O_3 were gained based on the weight ratio of akermanite/gehlenite. Then the MgO/Al_2O_3 weight ratio was calculated based on the above results. **Figure 13** shows the calculated results of MgO/Al_2O_3 weight ratio under different CaO/SiO_2 weight ratio of primary-slags. As shown in the picture the suitable MgO/Al_2O_3 weight ratio decreased with the increase of CaO/SiO_2 weight ratio, and this result could partly guide the burden optimization of blast furnace.

5. Conclusions

To evaluate the influence of high temperature interaction between sinter and lump ores, the softening and melting properties, the primary-slags formation behaviors of respective iron ores and integrated burdens were studied. Following conclusions were obtained from the above results.

(1) The high temperature interaction between sinter and lump ores would improve the primary-slags formation behaviors of integrated burdens, the formation temperature intervals, phase compositions, viscosity and fluidity indexes of primary-slags were all improved due to the high temperature interaction.

(2) The high temperature interaction index was influenced by the chemical composition and pore structures of iron ore samples. The INI index between lump ore L-2 and sinter was much higher due to the high porosity and high Al_2O_3, SiO_2 content of lump ore L-2.

(3) Though the softening and melting properties, primary-slags formation behaviors of lump ore L-2 was much worse than lump ore L-1, the high temperature properties of integrated burden B (consist of sinter and lump ore L-2) was not worse than that of integrated burden A (consist of sinter and lump ore L-1).

(4) The suitable MgO/Al_2O_3 weight ratio was calculated under the assumption that the only phases of slags were akermanite and gehlenite. The result shows that the MgO/Al_2O_3 weight ratio decreased with the increase of CaO/SiO_2 weight ratio.

Acknowledgement

The financial support of the National Natural Science Foundation of China (U1260202) and Specialized Research Fund for Doctoral Program of Higher Education (No. 20120006110002) is gratefully acknowledged.

REFERENCES

1) K. Sunahara, K. Nakano, M. Hoshi, T. Inada, S. Komatsu and T. Yamamoto: *ISIJ Int*., **48** (2008), 420.
2) T. Nishimura, K. Higuchi, M. Naito and K. Kunitomo: *ISIJ Int*., **51** (2011), 1316.
3) J. R. Kim, Y. S. Lee, D. J. Min, S. M. Jung and S. H. Yi: *ISIJ Int*., **44** (2004), 1291.
4) M. Hino, T. Nagasaka, A. Katsumata, K. I. Higuchi, K. Yamaguchi and N. Kon-no: *Metall. Mater. Trans. B*, **30B** (1999), 671.
5) Y. S. Lee, D. J. Min, S. M. Jung and S. H. Yi: *ISIJ Int*., **44** (2004), 1283.
6) S. L. Wu, G. J. Wang, W. Z. Jiang, J. Z. Sun and H. F. Xu: *Iron Steel* (*China*), **42** (2007), 11.
7) S. L. Wu, H. L. Han, H. F. Xu and L. J. Yan: *CIPE*, **10** (2010), 37.
8) S. L. Wu, H. L. Han, H. F. Xu, H. W. Wang and X. Q. Liu: *ISIJ Int*., **50** (2010), 686.
9) S. L. Wu, H. F. Xu and Y. Q. Tian: *Ironmaking Steelmaking*, **36** (2009), 19.
10) E. Kasai, S. Wu and Y. Omori: *Tetsu-to-Hagané*, **77** (1991), 56.
11) S. Wu, J. Du, H. Ma, Y. Tian and H. Xu: *J. Univ. Sci. Technol. B*, **27** (2005), 291.
12) H. Guo, J. L. Zhang, S. Z. Zhong, X. D. Zhang and W. Lv: *Iron Steel* (*China*), **43** (2008), 9.
13) C. E. Loo, L. T. Matthews and D. P. O'Dea: *ISIJ Int*., **51** (2011), 930.
14) W. Z. Tao and G. J. Wang: *Ironmaking* (*China*), **24** (2005), 46.
15) K. Higuchi, M. Naito, M. Nakano and Y. Takamoto: *ISIJ Int*., **44** (2004), 2057.
16) J. Z. Zhang: *Sintering Pelletizing* (*China*), **2** (1986), 12.
17) Y. Kashiwaya, T. Nakauchi, K. S. Pham, S. Akiyama and K. Ishi: *ISIJ Int*., **47** (2007), 44.
18) C. Fredericci, E. D. Zanotto and E. C. Ziemath: *J. Non-Cryst. Solids*, **273** (2000), 64.
19) L. Gan, C. X. Zhang, J. C. Zhou and Q. F. Shangguan: *J. Non-Cryst. Solids*, **358** (2012), 20.
20) P. Rocabois, J. N. Pontoire, J. Lehmann and H. Gaye: *J. Non-Cryst. Solids*, **282** (2001), 98.
21) Slag Atlas, 2nd ed., ed. by VDEh, Verlag Stahleisen GmbH, Düsseldorf, (1995), 111.
22) Slag Atlas, 2nd ed., ed. by VDEh, Verlag Stahleisen GmbH, Düsseldorf, (1995), 126.
23) X. Z. Zhao: The Principles of Transfer in Metallurgy, Metallurgical Industry Press, Beijing, (2004), 386.